

Triggering and quenching in the shadow of AGN: How does AGN proximity affect star formation in the EAGLE simulation?

Apashanka Das^{1,2*} and Biswajit Pandey^{1†}

¹ Department of Physics, Visva-Bharati University, Santiniketan, Birbhum, 731235, India

² Harish-Chandra Research Institute, HBNI, Chhatnag Road, Jhansi, Allahabad, 211109, India

July 14, 2025

Abstract

Active galactic nuclei (AGN) are among the most energetic phenomena in the universe, capable of regulating star formation in galaxies via radiative and mechanical feedback. While AGN feedback is well studied in host galaxies, its influence on neighbouring galaxies within the same large-scale environment remains less understood. In this work, we use the EAGLE cosmological hydrodynamical simulation to examine how proximity to AGN affects star formation in nearby star-forming galaxies (SFGs) out to 2 Mpc. A control sample matched in stellar mass and local density allows us to isolate AGN-driven environmental effects, quantified through the ΔSFR offset defined as the difference between a galaxy's star formation rate (SFR) and that of its matched controls. We find a significant and mass-dependent impact: 61% of AGN-adjacent SFGs show suppressed star formation, while 39% exhibit enhancement. Although the overall magnitude of these offsets is modest, the trends are statistically robust and consistent across the population. Suppression is prevalent in massive, gas-poor galaxies in high-mass halos, consistent with thermal feedback inhibiting gas cooling. Enhanced SFRs appear in low-mass, gas-rich galaxies, suggesting AGN-driven compression may locally trigger star formation. These trends emerge despite EAGLE implementing AGN feedback as a single-mode, stochastic thermal process, indicating that such models can reproduce both quenching and triggering regimes. Our findings demonstrate that AGN feedback extends well beyond host galaxies, impacting neighbouring systems in a non-uniform, distance-, mass-, and gas-dependent manner. This non-local AGN influence represents a critical, yet often overlooked, mechanism in shaping galaxy evolution within large-scale structures, bridging high-energy astrophysical processes and cosmic-scale environmental regulation.

Keywords: galaxies: galaxy evolution - AGN: AGN feedback - stars: star formation

1 Introduction

Active galactic nuclei (AGN) are among the most luminous sources in the universe, powered by accretion onto supermassive black holes (SMBHs) at the centers of galaxies. Their radiative output spanning from

*E-mail: a.das.cosmo@gmail.com

†E-mail: biswap@visva-bharati.ac.in (Corresponding author)

X-rays to radio wavelengths can reach luminosities as high as $10^{47} - 10^{48}$ erg/s (Fabian 1999; Woo and Urry 2002). This energetic feedback, arising from processes such as radiation pressure, jets, and winds, has a profound impact on the host galaxy and potentially on its surrounding environment. AGN-driven outflows and jets can heat or eject gas, regulate black hole growth, and suppress or even trigger star formation (Kawata and Gibson 2005; Wagner et al. 2013; Morganti 2017; Baron et al. 2018; Santoro et al. 2020). Such feedback is now considered a fundamental component of galaxy evolution models (Springel et al. 2005; Somerville et al. 2008; Kormendy and Ho 2013; Heckman and Best 2014; Harrison 2017), particularly for explaining the transition of galaxies from the star-forming “blue cloud” to the quiescent “red sequence” (Strateva et al. 2001; Blanton et al. 2003; Balogh et al. 2004; Baldry et al. 2004; Das and Pandey 2025).

Despite the near ubiquity of SMBHs in massive galaxies, only a fraction exhibit AGN activity at any given time. This raises important questions about what triggers AGN and how their effects propagate in space. A growing body of evidence suggests that AGN activity depends not only on internal factors such as gas availability, morphology, and bulge prominence (Ruffa et al. 2019; Shangquan et al. 2020; Ellison et al. 2021; Sampaio et al. 2023) but also on environmental influences. Observations indicate that AGN are more frequently found in massive galaxies residing in overdense regions, including groups and cluster outskirts (Lopes et al. 2017; Aird and Coil 2021), while some studies show enhanced AGN fractions in lower-density regions like voids (Ceccarelli et al. 2021). More recently, Banerjee et al. (2025) find that even at fixed stellar mass, AGN host galaxies exhibit statistically significant differences in colour, star formation rate, morphology, and stellar population age compared to star-forming galaxies, across both high- and low-density environments underscoring a possible role of assembly history in AGN activity. These apparent contradictions highlight the complexity of environmental triggering and regulation of AGN.

Of particular relevance is the possibility that AGN influence not only their host galaxies but also the surrounding intergalactic medium and nearby galaxies. Studies have shown that AGN can be more strongly clustered than star-forming galaxies (Gilli et al. 2009; Mandelbaum et al. 2009; Donoso et al. 2014; Hale et al. 2018; Singh et al. 2023), and the fraction of AGN tends to increase with decreasing distance to neighboring galaxies (Satyapal et al. 2014; Zhang et al. 2021). Such findings suggest a potential non-local impact of AGN activity, which may extend over several hundred kiloparsecs or more. This opens an important question: can AGN activity modulate star formation in neighbouring galaxies via environmental feedback? Recent discoveries of powerful radio-loud active galactic nuclei (AGN) (Hardcastle et al. 2019), including quasars and giant radio galaxies (GRGs) (Oei et al. 2023), underscore the far-reaching impact AGN activity can have on the surrounding cosmic environment. Dabhade et al. (2020) find that GRGs in their sample have sizes in the range $0.7 - 3.5$ Mpc. The record-breaking Alcyoneus whose radio jets extend over 5 Mpc (Oei et al. 2022) exemplify how AGN ejecta, powered by relativistic synchrotron emission, can influence regions well beyond their host halos. These immense structures interact with the intergalactic and circumgalactic medium on cosmological scales, injecting energy, redistributing magnetic fields, and potentially triggering or quenching star formation in nearby galaxies. The existence of such extended AGN structures raises a critical question: do these large-scale outflows leave a measurable imprint on neighbouring galaxies? While AGN feedback has traditionally been studied within the confines of the host galaxy, these observations demand a broader perspective, one that considers the environmental influence of AGNs on surrounding galaxies over megaparsec scales. Motivated by this, our study leverages the EAGLE (Evolution and Assembly of GaLaxies and their Environments) simulation (Schaye et al. 2015) to quantify how proximity to AGN-hosting galaxies affects star formation in neighbouring SFGs, thereby exploring the broader cosmic footprint of AGN feedback.

Understanding how AGN shape their cosmic environments requires a simulation that balances physical realism with statistical depth. The EAGLE simulation suite provides an ideal platform for probing the environmental influence of AGN on nearby galaxies. Its combination of cosmological volume, high-resolution hydrodynamics, and calibrated subgrid physics enables accurate modeling of AGN feed-

back and its impact on galaxy evolution. EAGLE’s well-resolved galaxy population and comprehensive database facilitate robust statistical comparisons, allowing us to isolate and quantify AGN-driven modulation of star formation beyond the host halo.

In this work, we take a statistical approach to investigate whether and how AGN can affect the star formation activity of galaxies in their immediate cosmic neighbourhood. Using the EAGLE simulation, we focus on star-forming galaxies located within 2 Mpc of AGN hosts and compare them to a carefully constructed control sample matched in stellar mass and local density. By computing the star formation rate offset (ΔSFR) for each galaxy relative to its controls, we aim to uncover whether proximity to AGN systematically enhances or suppresses star formation. This approach enables us to disentangle AGN-driven environmental effects from intrinsic galaxy properties, offering new insights into the non-local role of AGN feedback in galaxy evolution.

2 Data and Method of Analysis

2.1 EAGLE simulation data

In this study, we utilize data from the publicly available hydrodynamical simulation suite EAGLE (Schaye et al. 2015; Crain et al. 2015; McAlpine et al. 2016). The simulations are performed in periodic, cubic comoving volumes with side lengths ranging from 25 to 100 Mpc, and follow the evolution of both baryonic and dark matter particles from an initial redshift of $z = 127$ to the present day. EAGLE adopts a flat ΛCDM cosmology, calibrated using parameters from the *Planck* mission (Planck Collaboration et al. 2014), with $\Omega_\Lambda = 0.693$, $\Omega_m = 0.307$, $\Omega_b = 0.04825$, and $H_0 = 67.77 \text{ km s}^{-1} \text{ Mpc}^{-1}$.

We focus on the reference model Ref-L0100N1504, which simulates galaxy formation in a comoving box of length 100 Mpc, containing 2×1504^3 particles. In this model, the initial masses assigned to baryonic and dark matter particles are $1.81 \times 10^6 M_\odot$ and $9.70 \times 10^6 M_\odot$, respectively. Our analysis is restricted to the snapshot corresponding to redshift $z = 0$, and we include only well-resolved galaxies by applying the selection criterion $\text{Spurious} = 0$. This ensures the removal of artefacts with abnormally high black hole masses, low stellar mass, or anomalously high metallicity.

Key galaxy properties namely SFR and stellar mass are obtained from the Ref-L0100N1504-Aperture and Ref-L0100N1504-Magnitudes catalogs (Trayford et al. 2015; Doi et al. 2010). These values are measured within a 3D spherical aperture of 30 physical kpc centered on the location of the galaxy’s minimum gravitational potential, which provides observationally consistent estimates of galaxy properties (McAlpine et al. 2016). To ensure adequate resolution, we include only galaxies with $\log(M_{\text{stellar}}/M_{\text{sun}}) \geq 8.3$. This threshold guarantees that each galaxy is resolved by at least 110 baryonic particles.

2.2 Local density estimation

We characterize the local environment of each galaxy using the local density estimator η_k , defined using the k^{th} nearest neighbour method introduced by Casertano and Hut (1985):

$$\eta_k = \frac{k-1}{V(r_k)}, \quad (1)$$

where $V(r_k)$ is the volume of a sphere of radius r_k , the distance to the k^{th} nearest neighbour. We adopt $k = 5$ to compute the fifth-nearest neighbour density, η_5 , for each galaxy. To avoid underestimating densities near the simulation box boundaries, we exclude galaxies for which the distance to the boundary, r_b , is smaller than their fifth-nearest neighbour distance r_5 (i.e., $r_b < r_5$).

2.3 Identification of Star-Forming and AGN host galaxies in EAGLE

Galaxies hosting active galactic nuclei (AGN) emit radiation across the entire electromagnetic spectrum and appear significantly more luminous than normal star-forming galaxies. This enhanced luminosity arises from the accretion of matter onto a central supermassive black hole, adding a non-stellar radiative component to the galaxy’s total energy output. In contrast, the emission from SFGs originates primarily from stellar processes. AGN activity is also known to drive the transition of star-forming galaxies to quiescence by heating and removing gas, thus suppressing star formation. Emission line diagnostics can distinguish AGN from SFGs, as originally established by Baldwin et al. (1981).

In this work, we identify AGN hosts in the EAGLE simulation based on a bolometric luminosity threshold, following the approach of McAlpine et al. (2020). Galaxies with bolometric luminosity $L_{\text{bol}} \geq 10^{43} \text{ erg s}^{-1}$ are classified as AGN-active. The AGN bolometric luminosity is computed using

$$L_{\text{bol}} = \epsilon_r \dot{m}_{\text{BH}} c^2, \quad (2)$$

where $\epsilon_r = 0.1$ is the radiative efficiency of the accretion disk (Shakura and Sunyaev 1973), \dot{m}_{BH} is the black hole accretion rate, and c is the speed of light. This expression quantifies the fraction of accreted mass energy converted into radiation.

We also classify galaxies as actively star-forming if they satisfy a specific star formation rate (sSFR) threshold of $sSFR > 0.01 \text{ Gyr}^{-1}$, consistent with the criterion used in Schaye et al. (2015).

At redshift $z = 0$, our galaxy sample contains a total of 29,734 objects. Based on the criteria above, we identify the AGNs and SFGs in our sample (Table 1).

Table 1: Classification of galaxies at $z = 0$ in the EAGLE simulation based on star formation and AGN activity.

Galaxy Type	Selection criterion	Number of galaxies
Star-forming only	$sSFR > 0.01 \text{ Gyr}^{-1}$ and not AGN	17,589
AGN only	$L_{\text{bol}} \geq 10^{43} \text{ erg s}^{-1}$ and not star-forming	85
Star-forming AGN	Satisfies both criteria above	189
Quiescent non-AGN	Neither star-forming nor AGN	11,871
Total		29,734

AGN feedback, particularly in the so-called “radio mode”, is known to launch powerful jets that heat the circumgalactic medium, suppressing gas cooling in massive halos and leading to the quenching of star formation. While such internal feedback effects on the host galaxy are well studied, our focus is on exploring how AGN influence extends beyond the host halo specifically, how the presence of an AGN affects the physical properties of neighbouring galaxies.

To this end, we construct two comparison samples of star-forming galaxies:

- (i) those located within 2 Mpc of an AGN host galaxy, and
- (ii) those with no AGN in their surrounding environment out to 2 Mpc.

It is worth noting that our study considers only the 85 pure AGN host galaxies, ensuring a clean sample for isolating AGN-driven effects. To ensure a fair comparison, we perform control matching of these two samples in terms of stellar mass and local density, as described in the following subsection.

2.4 Constructing the control samples

The local environment of galaxies plays a key role in shaping their physical properties. It is well established that quiescent, red-sequence galaxies are more commonly found in high-density environments, while actively star-forming, blue-cloud galaxies dominate low-density regions. Several environmental processes such as ram pressure stripping, galaxy harassment, strangulation, and starvation become more efficient in overdense regions like galaxy clusters and groups, often leading to the suppression of star formation.

Stellar mass is another critical factor influencing star formation. Observational studies suggest that low-redshift galaxies can be broadly classified by a critical stellar mass of $\sim 3 \times 10^{10} M_{\text{sun}}$, above and below which galaxies exhibit distinct physical characteristics (Kauffmann et al. 2003). Hydrodynamical simulations and theoretical models link this mass threshold to a corresponding dark matter halo mass of $\sim 10^{12} M_{\text{sun}}$, which marks the transition from cold-mode to hot-mode gas accretion (Binney 2004; Birnboim and Dekel 2003; Dekel and Birnboim 2006; Kereš et al. 2005; Gabor et al. 2010; Gabor and Davé 2015).

Our sample includes 85 pure AGN, around which we identify a total of 1,757 star-forming galaxies located within a 2 Mpc radius. To ensure that comparisons of SFR between our target and reference samples are fair and unbiased, we construct a control sample that matches the stellar mass and local density of star-forming galaxies with neighbouring AGN. For each such galaxy, we identify five control galaxies from the population of star-forming galaxies that do not have any AGN within a 2 Mpc radius. The control galaxies are selected to match within 0.1 dex in stellar mass and 0.095 dex in local density. To confirm the statistical similarity of these samples, we perform a Kolmogorov–Smirnov (K–S) test. The null hypothesis that the two samples are drawn from the same parent distribution cannot be rejected at greater than 50% confidence for either mass or density, indicating that the matched samples are statistically indistinguishable.

While global comparisons between the two samples are informative, they can obscure individual deviations between a galaxy and its matched controls. To account for this, we compute a galaxy-by-galaxy offset metric, the SFR offset (ΔSFR), following the method of Patton et al. (2011). These offsets quantify how a given galaxy differs from its matched control galaxies, capturing individual-level deviations.

2.5 Mathematical definition of ΔSFR offsets

To quantify the relative star formation activity of SFGs in the vicinity of AGN, we adopt a differential metric known as the star formation rate offset, ΔSFR , following the approach of Patton et al. (2011). This metric captures the deviation in star formation activity of a given galaxy from the mean of a carefully selected control group. For each star-forming galaxy G located within a projected comoving distance of 2 Mpc from an AGN, we construct a control set $\mathcal{C}_G = \{C_1, C_2, \dots, C_5\}$ comprising five star-forming galaxies that lack a nearby AGN (within the same distance) and are closely matched in stellar mass (within ± 0.1 dex) and local galaxy density (within ± 0.095 dex). This matching ensures that the control galaxies share similar intrinsic and environmental properties, isolating AGN proximity as the primary variable.

The star formation rate offset for galaxy G is then defined as the difference between its own star formation rate, SFR_G , and the average SFR of its control set:

$$\Delta\text{SFR} = \text{SFR}_G - \left(\frac{1}{5} \sum_{i=1}^5 \text{SFR}_{C_i} \right). \quad (3)$$

By construction, a positive ΔSFR indicates that the galaxy is forming stars at an elevated rate relative to its peers, while a negative value reflects suppressed star formation. This galaxy-by-galaxy metric enables a precise and localized assessment of how AGN proximity modulates star formation, independent of confounding variables such as mass and environment.

3 Results

In this section, we present a detailed analysis of how proximity to AGN influences the star formation properties of neighbouring SFGs using the EAGLE simulation. We begin by comparing star formation activity between AGN-adjacent galaxies and a carefully matched control sample, followed by an examination of how these trends depend on stellar mass, halo mass, gas content, local density, and distance from the nearest AGN. Together, these analyses reveal a complex, mass-dependent, and spatially extended imprint of AGN feedback on the surrounding galaxy population.

3.1 Star formation offsets in galaxies near AGN

To quantify the impact of AGN on SFGs in their vicinity, we compute the SFR offset (ΔSFR) for each galaxy with an AGN within 2 Mpc, defined as the difference between its SFR and the average SFR of five control galaxies matched in stellar mass and local density. Figure 1 shows the stellar mass-SFR relation for these galaxies, split into two populations: those with $\Delta\text{SFR} < 0$ (left panel) and those with $\Delta\text{SFR} > 0$ (right panel). Both groups follow the general star-forming main sequence (SFMS), but with systematic deviations. Galaxies with suppressed SFR lie below the SFMS ridge, particularly at intermediate to high stellar masses, while galaxies with enhanced SFR are more prevalent at lower stellar masses and often lie above the SFMS. This suggests a mass-dependent influence of AGN on star formation activity.

To confirm that these differences arise from AGN proximity rather than selection bias, we examine the same relations for the corresponding control galaxies in Figure 2. Both control samples display consistent SFMS distributions, reinforcing that the observed suppression or enhancement is not due to differences in intrinsic properties, but rather reflects the environmental impact of nearby AGN.

We further assess the overall impact of AGN proximity on star formation by analyzing the distribution of ΔSFR across the full sample of AGN-adjacent galaxies, as shown in Figure 3. The median offset, $\Delta\text{SFR} = -0.0156$, indicates a mild yet statistically significant deviation in star formation activity relative to control galaxies matched in stellar mass and local density. Specifically, 61% of galaxies within 2 Mpc of an AGN exhibit negative ΔSFR values suggesting suppressed star formation while the remaining 39% show positive offsets, indicative of enhanced activity. These results reveal a subtle but pervasive shift away from the star-forming main sequence in both directions, depending on galaxy properties. This pattern supports the interpretation that AGN feedback acts as a regulatory mechanism not only within host galaxies but also on their surrounding environments. The small but consistent suppression observed may reflect low-level, widespread processes such as gentle gas heating or disruption of inflows, whereas enhancement in some systems could arise from mild gas compression or turbulence induced by AGN-driven outflows.

3.2 Mass dependence of AGN influence

To explore whether stellar or halo mass modulates the impact of AGN, we compare the mass distributions for the two AGN-adjacent populations in Figure 4. Galaxies with suppressed SFR tend to have higher stellar and halo masses, peaking at $\log(M_{\text{stellar}}/M_{\text{sun}}) \sim 10.2$ and $\log(M_{\text{halo}}/M_{\text{sun}}) \gtrsim 11$, while galaxies with enhanced SFR are predominantly low-mass systems in smaller halos (Figure 4). These findings

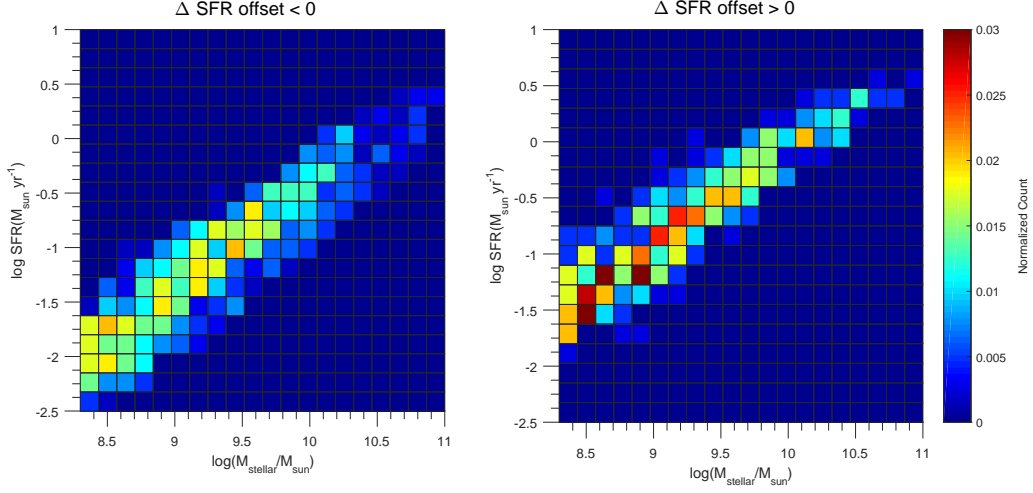


Figure 1: 2D PDFs showing the stellar mass-SFR relation for SFGs with nearby AGN. The left panel corresponds to galaxies with suppressed star formation ($\Delta\text{SFR} < 0$), while the right panel shows galaxies with enhanced star formation ($\Delta\text{SFR} > 0$), both defined relative to control galaxies matched in stellar mass and local density. The colourbar represents the normalized number count in each mass-SFR bin. While the main sequence is visible in both cases, galaxies with suppressed SFR tend to lie below the ridge line, particularly at higher stellar masses. In contrast, those with enhanced SFR show a concentration at lower masses and often lie above the main sequence, suggesting a mass-dependent AGN influence on neighbouring star formation activity.

support the idea that AGN are more effective at suppressing star formation in massive systems, where feedback mechanisms such as radio-mode jets and shock heating are more prominent. Conversely, in low-mass, gas-rich systems, AGN proximity may actually trigger star formation, potentially via mild compression of the surrounding medium.

3.3 Dependence on cold gas content and local environment

We next investigate whether cold gas availability and local density explain the divergent SFR responses. Figure 5 shows that galaxies with enhanced star formation have significantly higher cold gas masses, peaking near $\log(M_{\text{cold gas}}/M_{\odot}) \sim 9.5$, while the suppressed population is more gas-poor. This supports the interpretation that gas-rich galaxies are more susceptible to AGN-induced triggering, while gas-poor galaxies are more vulnerable to quenching. The local density distributions, however, are statistically indistinguishable between the two populations, confirming that our control-matching procedure effectively balanced environmental density. This reinforces the conclusion that observed differences in ΔSFR are primarily driven by AGN proximity, not local overdensity.

3.4 Gas-rich, low-mass galaxies and AGN-triggered star formation

Figure 6 shows the PDF of the stellar-to-cold gas mass ratio ($M_{\text{stellar}}/M_{\text{cold gas}}$) for star-forming galaxies with stellar mass $\log(M_{\text{stellar}}/M_{\text{sun}}) \leq 9.5$ and a positive ΔSFR offset, located within 2 Mpc of an AGN. The distribution peaks strongly below unity, indicating that the majority of these galaxies have more cold gas than stellar mass. This confirms that galaxies in this mass regime, despite their relatively small stellar

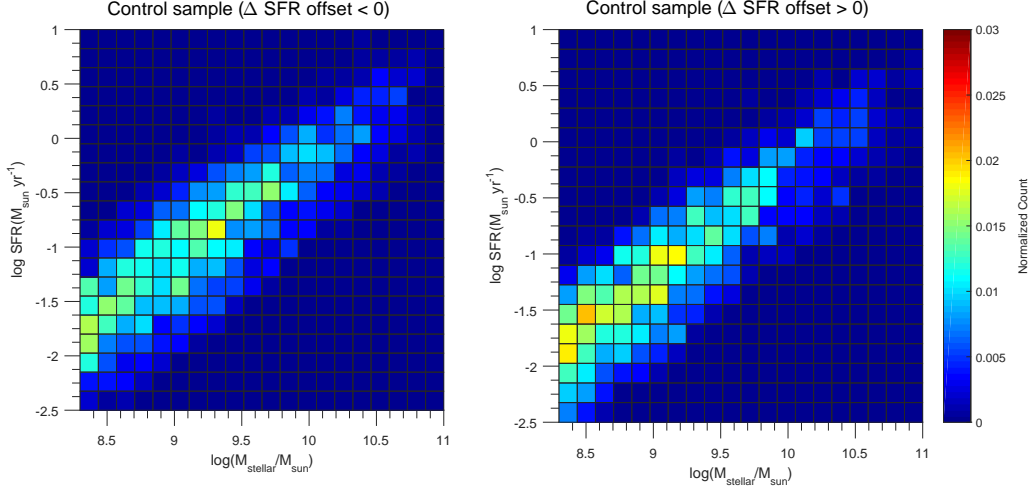


Figure 2: This shows the stellar mass-SFR relation for the matched control galaxies corresponding to the two AGN-affected star-forming populations shown in Figure 1. The left panel shows the control sample for galaxies with $\Delta\text{SFR} < 0$, and the right panel for those with $\Delta\text{SFR} > 0$. Both control populations display a consistent and well-defined SFMS, confirming that the underlying stellar mass and density distributions are statistically similar. The comparison with Figure 1 highlights that deviations from the main sequence in AGN-neighbouring galaxies arise due to environmental influence rather than intrinsic differences, underscoring the measurable non-local impact of AGN activity on star formation.

content, possess substantial cold gas reservoirs often exceeding $10^9 M_{\text{sun}}$ as previously shown in Figure 5.

While it might seem paradoxical that galaxies with low stellar mass can simultaneously host high cold gas content, this is consistent with both observations (Catinella et al. 2018) and hydrodynamical simulations (Davé et al. 2017), which find that low-mass star-forming galaxies commonly exhibit gas fractions greater than unity. Our results reinforce this picture and suggest that such gas-rich, low-mass galaxies are particularly susceptible to external perturbations from nearby AGN. The elevated gas content may provide a reservoir that, when compressed by AGN-driven outflows or turbulence in the surrounding medium, becomes primed for star formation enhancement.

These findings emphasize that it is not stellar mass alone, but the combination of gas content and environmental context, that governs a galaxy’s responsiveness to AGN proximity. In this light, the high gas-to-stellar mass ratios observed here offer a natural explanation for the star formation enhancement seen in low-mass galaxies near AGN hosts.

3.5 Radial dependence of star formation suppression and enhancement

Finally, we examine how the impact of AGN varies with distance. Figure 7 shows the median SFR of galaxies with suppressed ($\Delta\text{SFR} < 0$) and enhanced ($\Delta\text{SFR} > 0$) SFR as a function of their distance to the nearest AGN. Galaxies with suppressed SFR show markedly lower median values at separations $\lesssim 600$ kpc, while enhanced galaxies exhibit higher SFRs at similar distances. At separations beyond ~ 1.5 -2 Mpc, the median SFRs of both populations begin to converge, suggesting that the AGN influence is strongest within a few hundred kiloparsecs and weakens at larger scales. This radial dependence offers compelling evidence that AGN feedback effects extend beyond the host halo and influence the surrounding cosmic environment.

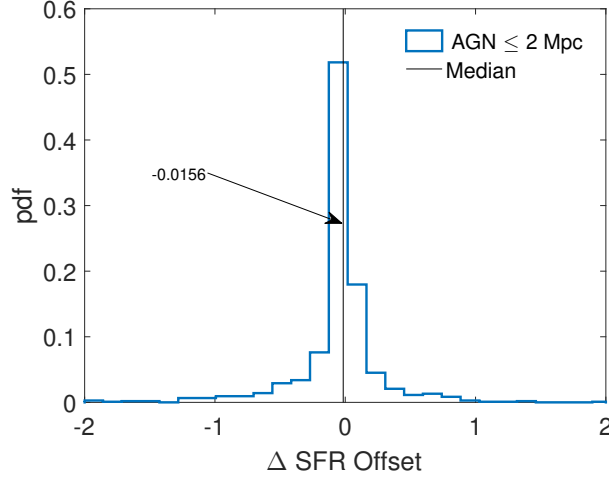


Figure 3: This shows the PDF of the ΔSFR offset for star-forming galaxies located within 2 Mpc of an AGN host. The ΔSFR offset is defined as the difference between the galaxy’s SFR and the mean SFR of five control galaxies matched in stellar mass and local density. The vertical dashed line indicates the median of the distribution, which is slightly negative at $\Delta\text{SFR} = -0.0156$, suggesting a mild suppression of star formation in AGN-neighbouring galaxies. The asymmetry of the distribution, with a longer tail toward negative offsets, supports the hypothesis that AGN feedback can suppress star formation in nearby galaxies, even beyond the host halo.

4 Conclusions

In this study, we have investigated the environmental impact of AGN on neighbouring SFGs using the EAGLE cosmological hydrodynamical simulation. Focusing on galaxies within 2 Mpc of an AGN host, we quantified the modulation of star formation activity by computing ΔSFR offsets relative to carefully matched control galaxies. Our analysis reveals that AGN proximity leaves a measurable and non-uniform imprint on the star-forming properties of nearby galaxies, extending well beyond the host halo and into the surrounding cosmic environment.

We find that the population of SFGs near AGN is bimodal: approximately 61% exhibit suppressed star formation compared to controls, while 39% show enhanced activity. This divergence is closely tied to galaxy mass and gas content. Galaxies with suppressed SFR tend to be more massive and reside in more massive halos, consistent with AGN feedback acting in concert with environmental quenching mechanisms to heat or expel gas, thereby reducing star formation. In contrast, galaxies with enhanced SFR are generally low-mass, gas-rich systems, suggesting that AGN-driven outflows or shocks may compress gas and stimulate star formation under favourable conditions.

Importantly, we show that these trends are not driven by differences in local density, as the environmental distributions of the suppressed and enhanced populations are statistically indistinguishable. The key differentiator is proximity to AGN, highlighting the non-local influence of AGN feedback on galaxy

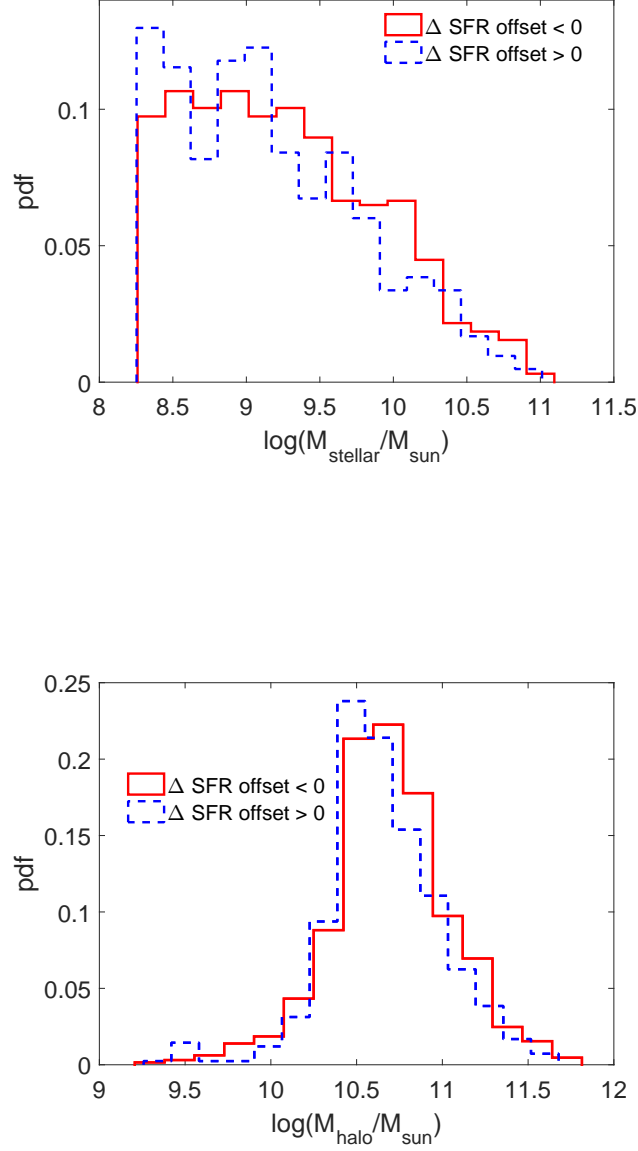


Figure 4: This shows the distributions of stellar mass (top panel) and halo mass (bottom panel) for SFGs located within 2 Mpc of an AGN, separated by whether they exhibit suppressed ($\Delta \text{SFR} < 0$) or enhanced ($\Delta \text{SFR} > 0$) star formation. Galaxies with suppressed SFR tend to have higher stellar masses, peaking at $\log(M_{\text{stellar}}/M_{\text{sun}}) \sim 10.2$, and reside in more massive halos ($\log(M_{\text{halo}}/M_{\text{sun}}) \gtrsim 11$). In contrast, galaxies with enhanced SFR are generally low-mass systems found in less massive halos. These trends suggest that the impact of AGN proximity on neighbouring galaxies is strongly modulated by both stellar and halo mass.

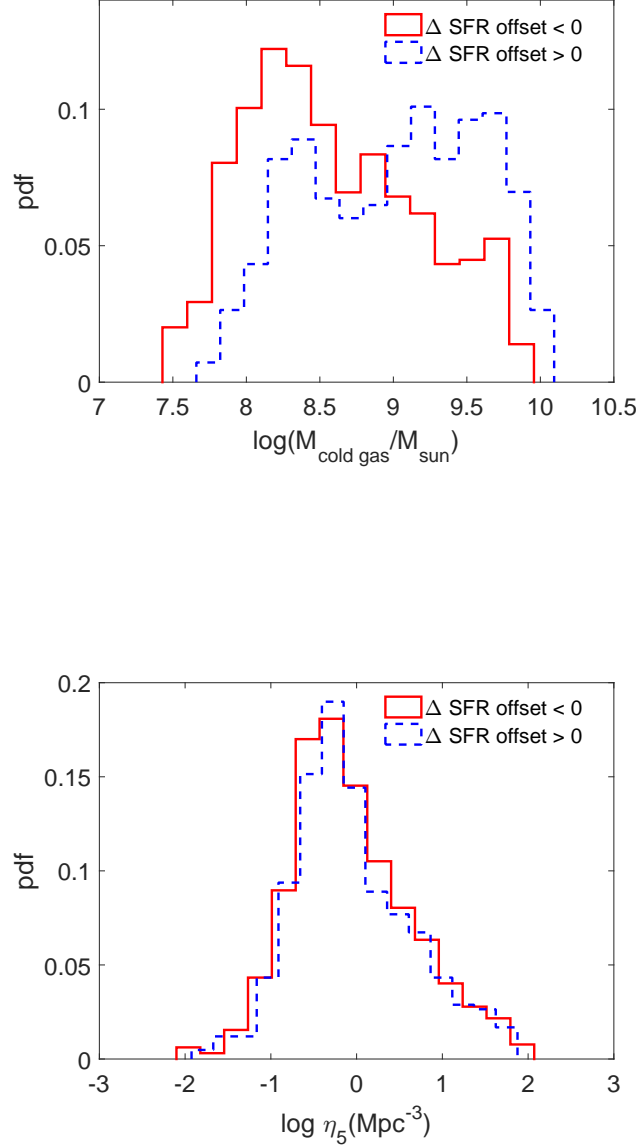


Figure 5: This shows the distributions of cold gas mass (top panel) and local environmental density (bottom panel) for SFGs located within 2 Mpc of an AGN, divided by whether they show suppressed ($\Delta \text{SFR} < 0$) or enhanced ($\Delta \text{SFR} > 0$) star formation. Galaxies with enhanced SFR tend to have significantly higher cold gas content, peaking near $\log(M_{\text{cold gas}}/M_{\odot}) \sim 9.5$, while those with suppressed SFR peak at lower gas masses. The local density distributions of both populations are statistically indistinguishable, confirming that environmental density was effectively controlled. This strengthens the conclusion that differences in ΔSFR are primarily driven by AGN influence rather than large-scale environmental effects.

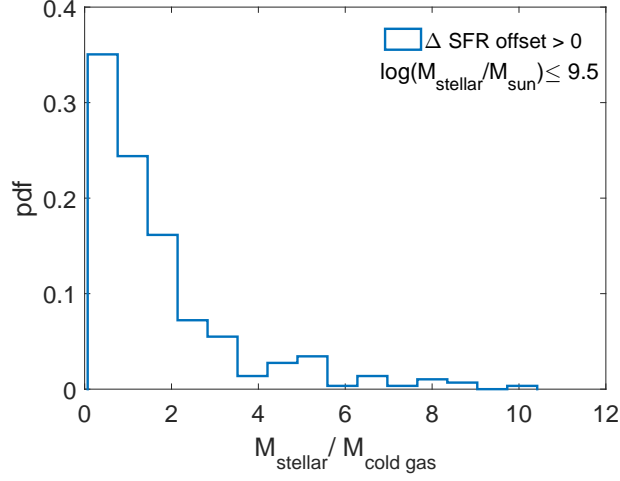


Figure 6: This shows the PDF of the stellar-to-cold gas mass ratio ($M_{\text{stellar}}/M_{\text{cold gas}}$) for star-forming galaxies with stellar mass $\log(M_{\text{stellar}}/M_{\text{sun}}) \leq 9.5$ and positive star formation rate offsets ($\Delta\text{SFR} > 0$), located within 2 Mpc of an AGN. The distribution peaks strongly below unity, indicating that most of these low-mass galaxies are gas-rich, with cold gas masses exceeding their stellar mass. When combined with the earlier result that galaxies with $\Delta\text{SFR} > 0$ tend to have $M_{\text{gas}} > 10^9 M_{\text{sun}}$, this suggests that gas-rich, low-mass galaxies may be particularly prone to AGN-triggered star formation, likely due to their sensitivity to gas compression or turbulence in AGN-influenced environments.

evolution. Moreover, we observe a strong radial dependence: the median SFR of AGN-adjacent galaxies differs most significantly from controls at separations less than ~ 600 kpc, with both suppression and enhancement effects diminishing beyond ~ 1 Mpc.

Together, these findings demonstrate that AGN can regulate not only their host galaxies but also exert meaningful influence on star formation in neighbouring systems across cosmological scales. This environmental AGN feedback adds an important dimension to our understanding of galaxy evolution, particularly in explaining the spatially extended quenching and triggering of star formation. Our results emphasize the need for models of galaxy evolution to incorporate both local and large-scale AGN effects when interpreting the role of feedback in shaping the star-forming galaxies.

Our main findings are summarized as follows:

- (i) Approximately 61% of star-forming galaxies with nearby AGNs exhibit suppressed star formation, while the remaining 39% show enhanced activity relative to matched control galaxies.
- (ii) Star formation enhancement is more prevalent in low-mass, gas-rich systems ($M_{\text{stellar}} < 10^{9.5} M_{\text{sun}}$), whereas suppression dominates in more massive galaxies with reduced cold gas content.
- (iii) Galaxies with suppressed SFRs tend to reside in slightly more massive dark matter halos than those with enhanced SFRs.

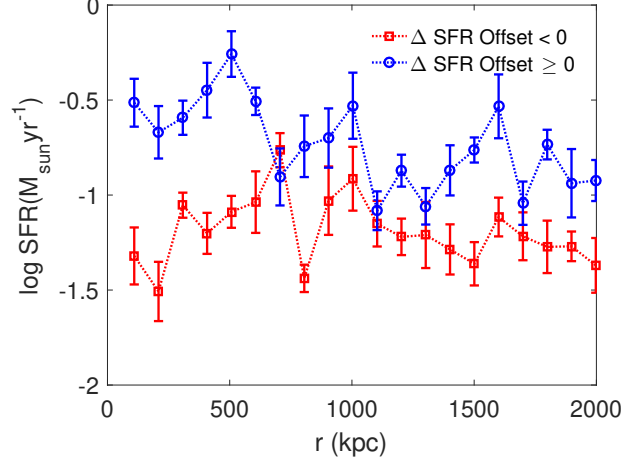


Figure 7: This shows the median SFR of star-forming galaxies as a function of their projected physical distance from the nearest AGN, limited to separations within 2 Mpc. The two curves represent galaxies with suppressed ($\Delta\text{SFR} < 0$) and enhanced ($\Delta\text{SFR} > 0$) star formation relative to matched control galaxies with no nearby AGN. One-sigma jackknife error bars are shown to indicate the statistical uncertainty. Galaxies with suppressed SFR exhibit significantly lower median SFRs, particularly within ~ 600 kpc, while those with enhanced SFR maintain higher values at small separations. This distance-dependent behaviour suggests that AGN feedback can influence neighbouring galaxies across substantial scales, with stronger effects at smaller separations.

- (iv) The local density distributions of the suppressed and enhanced populations are statistically indistinguishable, supporting the interpretation that AGN proximity rather than large-scale environment drives the observed trends.
- (v) Star formation modulation is most pronounced within ~ 600 kpc of AGNs, suggesting a clear radial dependence of AGN influence on neighbouring galaxies.

Our results offer new insights into the spatially extended impact of AGN feedback on surrounding galaxies, building on and expanding the findings of previous studies using the EAGLE simulation. It is important to note that EAGLE models AGN feedback using a single-mode, stochastic thermal injection scheme (Schaye et al. 2015), which does not explicitly distinguish between quasar- and radio-mode feedback. Despite this simplification, the simulation successfully reproduces a broad range of observational properties, suggesting that this unified thermal mode captures the essential physics of AGN-driven quenching.

Wright et al. (2019) demonstrated that AGN activity in massive satellites contributes to shortened quenching timescales, primarily through thermal heating that removes or prevents the cooling of gas. Similarly, Visser-Zadvornyi et al. (2025) argue that quenching in satellites is governed by the interplay between AGN heating and the absence of fresh gas accretion, resulting in exhaustion of the interstellar medium (ISM). Our findings support and extend these conclusions by showing that AGN influence is not

confined to host galaxies or satellites alone, but can propagate outward to affect star formation in neighbouring galaxies on scales up to ~ 1 Mpc. This broadens the known reach of AGN feedback, indicating that it may play a previously underappreciated role in shaping the star formation histories of galaxies in the same environment.

Furthermore, while Bluck et al. (2023) find that black hole mass and the potential well depth strongly predict AGN-driven quenching in central galaxies, our results provide complementary evidence that proximity to AGN regardless of host properties can influence SFRs in external galaxies. This introduces an environmental dimension to AGN feedback that is not captured by studies focused solely on internal galaxy properties.

Our findings are consistent with those of Goubert et al. (2024), who show that quiescence in massive galaxies whether centrals or high-mass satellites is primarily governed by intrinsic properties such as black hole mass, while low-mass satellite quenching is more strongly influenced by environmental factors like halo mass or local density. Building on this framework, our results demonstrate that proximity to AGN can further modulate star formation in gas-rich, low-mass systems, suggesting a role for AGN-induced environmental feedback in accelerating or even triggering quenching in this regime. This interpretation is further supported by the work of Dashyan et al. (2019), who find that AGN feedback from central galaxies can significantly reduce the gas content and suppress star formation in their satellites, with detectable effects extending out to several virial radii. Together, these studies reinforce the view that AGN feedback operates not only within host galaxies but also exerts non-local, environmentally mediated influence on surrounding galaxies across large scales.

Crucially, our work highlights a mass- and gas-dependent bifurcation in AGN influence: galaxies with high stellar and halo mass are more likely to experience star formation suppression, consistent with thermal AGN heating preventing gas cooling whereas low-mass, gas-rich galaxies near AGN can show enhanced SFRs, suggesting the possibility of positive feedback via shock compression or turbulence in the surrounding medium. These dual trends emerge despite EAGLE modeling only quasar-mode feedback, implying that even a single-mode AGN model can reproduce both suppressive and stimulative effects in different regimes.

In summary, our study demonstrates that AGN feedback though implemented in EAGLE as a single-mode thermal process can produce nuanced, environment-wide signatures in galaxy populations. By extending the scope of AGN impact beyond the host to neighbouring galaxies, and by uncovering distinct pathways for suppression and enhancement of star formation depending on galaxy mass and gas content, we provide new evidence for the non-local, environmentally mediated nature of AGN feedback.

Further studies, particularly those combining simulations with observational data from JWST (Gardner et al. 2006), SKA (Dewdney et al. 2009), or Euclid (Euclid Collaboration et al. 2025), will be essential in constraining the physical mechanisms responsible for these trends and improving our understanding of galaxy evolution in AGN-dominated environments.

5 Acknowledgements

AD acknowledges Harish-Chandra Research Institute, Allahabad for providing support through a post-doctoral fellowship. BP acknowledges the support provided by IUCAA, Pune, through an associateship programme and ICARD, Visva-Bharati. The authors extend their gratitude to the Virgo Consortium for providing public access to their simulation data. The EAGLE simulations were performed using the DiRAC-2 facility at Durham, managed by the ICC, and the PRACE facility Curie based in France at TGCC, CEA, Bruyères-le-Châtel.

6 Data availability

The EAGLE simulation data used in this study are publicly available through the EAGLE database at <https://icc.dur.ac.uk/Eagle/database.php>. Additional data products generated and analyzed during this work are available from the authors upon reasonable request.

References

- J. Aird and A. L. Coil. The AGN-galaxy-halo connection: the distribution of AGN host halo masses to $z = 2.5$. *MNRAS*, 502(4):5962–5980, Apr. 2021. doi: 10.1093/mnras/stab312. 2
- I. K. Baldry, K. Glazebrook, J. Brinkmann, Ž. Ivezić, R. H. Lupton, R. C. Nichol, and A. S. Szalay. Quantifying the Bimodal Color-Magnitude Distribution of Galaxies. *ApJ*, 600(2):681–694, Jan. 2004. doi: 10.1086/380092. 2
- J. A. Baldwin, M. M. Phillips, and R. Terlevich. Classification parameters for the emission-line spectra of extragalactic objects. *Publications of the Astronomical Society of the Pacific*, 93:5–19, Feb. 1981. doi: 10.1086/130766. 4
- M. L. Balogh, I. K. Baldry, R. Nichol, C. Miller, R. Bower, and K. Glazebrook. The Bimodal Galaxy Color Distribution: Dependence on Luminosity and Environment. *ApJ Letters*, 615(2):L101–L104, Nov. 2004. doi: 10.1086/426079. 2
- A. Banerjee, B. Pandey, and A. Nandi. Clustering and physical properties of AGN and Star-Forming Galaxies at fixed stellar mass: does assembly bias have a role in AGN activity? *PASA*, 42(78):1–16, June 2025. doi: 10.1017/pasa.2025.10052. 2
- D. Baron, H. Netzer, J. X. Prochaska, Z. Cai, S. Cantalupo, D. C. Martin, M. Matuszewski, A. M. Moore, P. Morrissey, and J. D. Neill. Direct evidence of AGN feedback: a post-starburst galaxy stripped of its gas by AGN-driven winds. *MNRAS*, 480(3):3993–4016, Nov. 2018. doi: 10.1093/mnras/sty2113. 2
- J. Binney. On the origin of the galaxy luminosity function. *MNRAS*, 347(4):1093–1096, Feb. 2004. doi: 10.1111/j.1365-2966.2004.07277.x. 5
- Y. Birnboim and A. Dekel. Virial shocks in galactic haloes? *MNRAS*, 345(1):349–364, Oct. 2003. doi: 10.1046/j.1365-8711.2003.06955.x. 5
- M. R. Blanton, D. W. Hogg, N. A. Bahcall, I. K. Baldry, J. Brinkmann, I. Csabai, D. Eisenstein, M. Fukugita, J. E. Gunn, Ž. Ivezić, D. Q. Lamb, R. H. Lupton, J. Loveday, J. A. Munn, R. C. Nichol, S. Okamura, D. J. Schlegel, K. Shimasaku, M. A. Strauss, M. S. Vogeley, and D. H. Weinberg. The Broadband Optical Properties of Galaxies with Redshifts $0.02 < z < 0.22$. *ApJ*, 594(1):186–207, Sept. 2003. doi: 10.1086/375528. 2
- A. F. L. Bluck, J. M. Piotrowska, and R. Maiolino. The Fundamental Signature of Star Formation Quenching from AGN Feedback: A Critical Dependence of Quiescence on Supermassive Black Hole Mass, Not Accretion Rate. *ApJ*, 944(1):108, Feb. 2023. doi: 10.3847/1538-4357/acac7c. 14
- S. Casertano and P. Hut. Core radius and density measurements in N-body experiments Connections with theoretical and observational definitions. *ApJ*, 298:80–94, Nov. 1985. doi: 10.1086/163589. 3
- B. Catinella, A. Saintonge, S. Janowiecki, L. Cortese, R. Davé, J. J. Lemonias, A. P. Cooper, D. Schiminovich, C. B. Hummels, S. Fabello, K. Geréb, V. Kilborn, and J. Wang. xGASS: total cold gas scaling relations and molecular-to-atomic gas ratios of galaxies in the local Universe. *MNRAS*, 476(1):875–895, May 2018. doi: 10.1093/mnras/sty089. 8

- L. Ceccarelli, F. Duplancic, and D. Garcia Lambas. The impact of void environment on AGN. *MNRAS*, 509(2):1805–1819, Nov. 2021. doi: 10.1093/mnras/stab2902. 2
- R. A. Crain, J. Schaye, R. G. Bower, M. Furlong, M. Schaller, T. Theuns, C. Dalla Vecchia, C. S. Frenk, I. G. McCarthy, J. C. Helly, A. Jenkins, Y. M. Rosas-Guevara, S. D. M. White, and J. W. Trayford. The EAGLE simulations of galaxy formation: calibration of subgrid physics and model variations. *MNRAS*, 450(2):1937–1961, June 2015. doi: 10.1093/mnras/stv725. 3
- P. Dabhade, H. J. A. Röttgering, J. Bagchi, T. W. Shimwell, M. J. Hardcastle, S. Sankhyayan, R. Morganti, M. Jamrozy, A. Shulevski, and K. J. Duncan. Giant radio galaxies in the LOFAR Two-metre Sky Survey. I. Radio and environmental properties. *A&A*, 635:A5, Mar. 2020. doi: 10.1051/0004-6361/201935589. 2
- A. Das and B. Pandey. The long road to the Green Valley: Tracing the evolution of the Green Valley galaxies in the EAGLE simulation. *JCAP*, 2025(5):101, May 2025. doi: 10.1088/1475-7516/2025/05/101. 2
- G. Dashyan, E. Choi, R. S. Somerville, T. Naab, A. C. N. Quirk, M. Hirschmann, and J. P. Ostriker. AGN-driven quenching of satellite galaxies. *MNRAS*, 487(4):5889–5901, Aug. 2019. doi: 10.1093/mnras/stz1697. 14
- R. Davé, M. H. Rafieferantsoa, R. J. Thompson, and P. F. Hopkins. MUFASA: Galaxy star formation, gas, and metal properties across cosmic time. *MNRAS*, 467(1):115–132, May 2017. doi: 10.1093/mnras/stx108. 8
- A. Dekel and Y. Birnboim. Galaxy bimodality due to cold flows and shock heating. *MNRAS*, 368(1):2–20, May 2006. doi: 10.1111/j.1365-2966.2006.10145.x. 5
- P. E. Dewdney, P. J. Hall, R. T. Schilizzi, and T. J. L. W. Lazio. The Square Kilometre Array. *IEEE Proceedings*, 97(8):1482–1496, Aug. 2009. doi: 10.1109/JPROC.2009.2021005. 14
- M. Doi, M. Tanaka, M. Fukugita, J. E. Gunn, N. Yasuda, Ž. Ivezić, J. Brinkmann, E. de Haars, S. J. Kleinman, J. Krzesinski, and R. French Leger. Photometric Response Functions of the Sloan Digital Sky Survey Imager. *AJ*, 139(4):1628–1648, Apr. 2010. doi: 10.1088/0004-6256/139/4/1628. 3
- E. Donoso, L. Yan, D. Stern, and R. J. Assef. The Angular Clustering of WISE-selected Active Galactic Nuclei: Different Halos for Obscured and Unobscured Active Galactic Nuclei. *ApJ*, 789(1):44, July 2014. doi: 10.1088/0004-637X/789/1/44. 2
- S. L. Ellison, T. Wong, S. F. Sánchez, D. Colombo, A. Bolatto, J. Barrera-Ballesteros, R. García-Benito, V. Kalinova, Y. Luo, M. Rubio, and S. N. Vogel. The EDGE-CALIFA survey: central molecular gas depletion in AGN host galaxies - a smoking gun for quenching? *MNRAS*, 505(1):L46–L51, July 2021. doi: 10.1093/mnras/slab047. 2
- Euclid Collaboration, Y. Mellier, Abdurro’uf, J. A. Acevedo Barroso, A. Achúcarro, J. Adamek, R. Adam, G. E. Addison, N. Aghanim, M. Agüena, V. Ajani, Y. Akrami, A. Al-Bahlawan, A. Alavi, I. S. Albuquerque, G. Alestas, G. Alguero, A. Allaoui, S. W. Allen, V. Allevato, A. V. Alonso-Tetilla, B. Altieri, A. Alvarez-Candal, S. Alvi, A. Amara, L. Amendola, J. Amiaux, I. T. Andika, S. Andreon, A. Andrews, G. Angora, R. E. Angulo, F. Annibali, A. Anselmi, S. Anselmi, S. Arcari, M. Archidiacono, G. Aricò, M. Arnaud, S. Arnouts, M. Asgari, J. Asorey, L. Atayde, H. Atek, F. Atrio-Barandela, M. Aubert, E. Aubourg, T. Auphan, N. Auricchio, B. Aussel, H. Aussel, P. P. Avelino, A. Avgoustidis, S. Avila, S. Awan, R. Azzollini, C. Baccigalupi, E. Bachelet, D. Bacon, M. Baes, M. B. Bagley, B. Bahr-Kalus, A. Balaguera-Antolinez, E. Balbinot, M. Balcells, M. Baldi, I. Baldry, A. Balestra,

- M. Ballardini, O. Ballester, M. Balogh, E. Bañados, R. Barbier, S. Bardelli, M. Baron, T. Barreiro, R. Barrena, J. C. Barriere, B. J. Barros, A. Barthelemy, N. Bartolo, A. Basset, P. Battaglia, A. J. Battisti, C. M. Baugh, L. Baumont, L. Bazzanini, J. P. Beaulieu, V. Beckmann, A. N. Belikov, J. Bel, F. Bellagamba, M. Bella, E. Bellini, K. Benabed, R. Bender, G. Benevento, C. L. Bennett, K. Benson, P. Bergamini, J. R. Bermejo-Climent, F. Bernardeau, D. Bertacca, M. Berthe, J. Berthier, M. Bethermin, F. Beutler, C. Bevilhon, S. Bhargava, R. Bhatawdekar, D. Bianchi, L. Bisigello, A. Biviano, R. P. Blake, A. Blanchard, J. Blazek, L. Blot, A. Bosco, C. Bodendorf, T. Boenke, H. Böhringer, P. Boldrini, M. Bolzonella, A. Bonchi, M. Bonici, D. Bonino, L. Bonino, C. Bonvin, W. Bon, J. T. Booth, S. Borgani, A. S. Borlaff, E. Borsato, B. Bose, M. T. Botticella, A. Boucaud, F. Bouche, J. S. Boucher, D. Boutigny, T. Bouvard, R. Bouwens, H. Bouy, R. A. A. Bowler, V. Bozza, E. Bozzo, E. Branchini, G. Brando, S. Brau-Nogue, P. Brekke, M. N. Bremer, M. Brescia, M. A. Breton, J. Brinchmann, T. Brinckmann, C. Brockley-Blatt, M. Brodwin, L. Brouard, M. L. Brown, S. Bruton, J. Bucko, H. Budelmeijer, G. Buenadicha, F. Buitrago, P. Burger, C. Burigana, V. Busillo, D. Busonero, R. Cabanac, L. Cabayol-Garcia, M. S. Cagliari, A. Caillat, L. Caillat, M. Calabrese, A. Calabro, G. Calderone, F. Calura, B. Camacho Quevedo, S. Camera, L. Campos, G. Cañas-Herrera, G. P. Candini, M. Cantiello, V. Capobianco, E. Cappellaro, N. Cappelluti, A. Cappi, K. I. Caputi, C. Cara, C. Carbone, V. F. Cardone, E. Carella, R. G. Carlberg, M. Carle, L. Carminati, F. Caro, J. M. Carrasco, J. Carretero, P. Carrilho, J. Carron Duque, and B. Carry. Euclid: I. Overview of the Euclid mission. *A&A*, 697:A1, May 2025. doi: 10.1051/0004-6361/202450810. 14
- A. C. Fabian. Active Galactic Nuclei. *Proceedings of the National Academy of Science*, 96(9):4749–4751, Apr. 1999. doi: 10.1073/pnas.96.9.4749. 2
- J. M. Gabor and R. Davé. Hot gas in massive haloes drives both mass quenching and environment quenching. *MNRAS*, 447(1):374–391, Feb. 2015. doi: 10.1093/mnras/stu2399. 5
- J. M. Gabor, R. Davé, K. Finlator, and B. D. Oppenheimer. How is star formation quenched in massive galaxies? *MNRAS*, 407(2):749–771, Sept. 2010. doi: 10.1111/j.1365-2966.2010.16961.x. 5
- J. P. Gardner, J. C. Mather, M. Clampin, R. Doyon, M. A. Greenhouse, H. B. Hammel, J. B. Hutchings, P. Jakobsen, S. J. Lilly, K. S. Long, J. I. Lunine, M. J. McCaughrean, M. Mountain, J. Nella, G. H. Rieke, M. J. Rieke, H.-W. Rix, E. P. Smith, G. Sonneborn, M. Stiavelli, H. S. Stockman, R. A. Windhorst, and G. S. Wright. The James Webb Space Telescope. *Space Science Reviews*, 123(4):485–606, Apr. 2006. doi: 10.1007/s11214-006-8315-7. 14
- R. Gilli, G. Zamorani, T. Miyaji, J. Silverman, M. Brusa, V. Mainieri, N. Cappelluti, E. Daddi, C. Porciani, L. Pozzetti, F. Civano, A. Comastri, A. Finoguenov, F. Fiore, M. Salvato, C. Vignali, G. Hasinger, S. Lilly, C. Impey, J. Trump, P. Capak, H. McCracken, N. Scoville, Y. Taniguchi, C. M. Carollo, T. Contini, J. P. Kneib, O. Le Fevre, A. Renzini, M. Scodeggio, S. Bardelli, M. Bolzonella, A. Bongiorno, K. Caputi, A. Cimatti, G. Coppia, O. Cucciati, S. de La Torre, L. de Ravel, P. Franzetti, B. Garilli, A. Iovino, P. Kampeczyk, C. Knobel, K. Kovač, F. Lamareille, J. F. Le Borgne, V. Le Brun, C. Maier, M. Mignoli, R. Pellò, Y. Peng, E. Perez Montero, E. Ricciardelli, M. Tanaka, L. Tasca, L. Tresse, D. Vergani, E. Zucca, U. Abbas, D. Bottini, A. Cappi, P. Cassata, M. Fumana, L. Guzzo, A. Leauthaud, D. Maccagni, C. Marinoni, P. Memeo, B. Meneux, P. Oesch, R. Scaramella, and J. Walcher. The spatial clustering of X-ray selected AGN in the XMM-COSMOS field. *A&A*, 494(1):33–48, Jan. 2009. doi: 10.1051/0004-6361:200810821. 2
- P. H. Goubert, A. F. L. Bluck, J. M. Piotrowska, and R. Maiolino. The role of environment and AGN feedback in quenching local galaxies: comparing cosmological hydrodynamical simulations to the SDSS. *MNRAS*, 528(3):4891–4921, Mar. 2024. doi: 10.1093/mnras/stae269. 14

- C. L. Hale, M. J. Jarvis, I. Delvecchio, P. W. Hatfield, M. Novak, V. Smolčić, and G. Zamorani. The clustering and bias of radio-selected AGN and star-forming galaxies in the COSMOS field. *MNRAS*, 474(3):4133–4150, Mar. 2018. doi: 10.1093/mnras/stx2954. 2
- M. J. Hardcastle, W. L. Williams, P. N. Best, J. H. Croston, K. J. Duncan, H. J. A. Röttgering, J. Sabater, T. W. Shimwell, C. Tasse, J. R. Callingham, R. K. Cochrane, F. de Gasperin, G. Gürkan, M. J. Jarvis, V. Mahatma, G. K. Miley, B. Mingo, S. Mooney, L. K. Morabito, S. P. O’Sullivan, I. Prandoni, A. Shulevski, and D. J. B. Smith. Radio-loud AGN in the first LoTSS data release. The lifetimes and environmental impact of jet-driven sources. *A&A*, 622:A12, Feb. 2019. doi: 10.1051/0004-6361/201833893. 2
- C. M. Harrison. Impact of supermassive black hole growth on star formation. *Nature Astronomy*, 1:0165, July 2017. doi: 10.1038/s41550-017-0165. 2
- T. M. Heckman and P. N. Best. The Coevolution of Galaxies and Supermassive Black Holes: Insights from Surveys of the Contemporary Universe. *Annual Review of Astronomy and Astrophysics*, 52:589–660, Aug. 2014. doi: 10.1146/annurev-astro-081913-035722. 2
- G. Kauffmann, T. M. Heckman, S. D. M. White, S. Charlot, C. Tremonti, E. W. Peng, M. Seibert, J. Brinkmann, R. C. Nichol, M. SubbaRao, and D. York. The dependence of star formation history and internal structure on stellar mass for 10^5 low-redshift galaxies. *MNRAS*, 341(1):54–69, May 2003. doi: 10.1046/j.1365-8711.2003.06292.x. 5
- D. Kawata and B. K. Gibson. Self-regulated active galactic nuclei heating in elliptical galaxies. *MNRAS*, 358(1):L16–L20, Mar. 2005. doi: 10.1111/j.1745-3933.2005.00018.x. 2
- D. Kereš, N. Katz, D. H. Weinberg, and R. Davé. How do galaxies get their gas? *MNRAS*, 363(1):2–28, Oct. 2005. doi: 10.1111/j.1365-2966.2005.09451.x. 5
- J. Kormendy and L. C. Ho. Coevolution (Or Not) of Supermassive Black Holes and Host Galaxies. *Annual Review of Astronomy and Astrophysics*, 51(1):511–653, Aug. 2013. doi: 10.1146/annurev-astro-082708-101811. 2
- P. A. A. Lopes, A. L. B. Ribeiro, and S. B. Rembold. NoSOCS in SDSS - VI. The environmental dependence of AGN in clusters and field in the local Universe. *MNRAS*, 472(1):409–418, Nov. 2017. doi: 10.1093/mnras/stx2046. 2
- R. Mandelbaum, C. Li, G. Kauffmann, and S. D. M. White. Halo masses for optically selected and for radio-loud AGN from clustering and galaxy-galaxy lensing. *MNRAS*, 393(2):377–392, Feb. 2009. doi: 10.1111/j.1365-2966.2008.14235.x. 2
- S. McAlpine, J. C. Helly, M. Schaller, J. W. Trayford, Y. Qu, M. Furlong, R. G. Bower, R. A. Crain, J. Schaye, T. Theuns, C. Dalla Vecchia, C. S. Frenk, I. G. McCarthy, A. Jenkins, Y. Rosas-Guevara, S. D. M. White, M. Baes, P. Camps, and G. Lemson. The EAGLE simulations of galaxy formation: Public release of halo and galaxy catalogues. *Astronomy and Computing*, 15:72–89, Apr. 2016. doi: 10.1016/j.ascom.2016.02.004. 3
- S. McAlpine, C. M. Harrison, D. J. Rosario, D. M. Alexander, S. L. Ellison, P. H. Johansson, and D. R. Patton. Galaxy mergers in EAGLE do not induce a significant amount of black hole growth yet do increase the rate of luminous AGN. *MNRAS*, 494(4):5713–5733, June 2020. doi: 10.1093/mnras/staa1123. 4
- R. Morganti. The many routes to AGN feedback. *Frontiers in Astronomy and Space Sciences*, 4:42, Nov. 2017. doi: 10.3389/fspas.2017.00042. 2

- M. S. S. L. Oei, R. J. van Weeren, M. J. Hardcastle, A. Botteon, T. W. Shimwell, P. Dabhade, A. R. D. J. G. I. B. Gast, H. J. A. Röttgering, M. Brüggen, C. Tasse, W. L. Williams, and A. Shulevski. The discovery of a radio galaxy of at least 5 Mpc. *A&A*, 660:A2, Apr. 2022. doi: 10.1051/0004-6361/202142778. 2
- M. S. S. L. Oei, R. J. van Weeren, A. R. D. J. G. I. B. Gast, A. Botteon, M. J. Hardcastle, P. Dabhade, T. W. Shimwell, H. J. A. Röttgering, and A. Drabent. Measuring the giant radio galaxy length distribution with the LoTSS. *A&A*, 672:A163, Apr. 2023. doi: 10.1051/0004-6361/202243572. 2
- D. R. Patton, S. L. Ellison, L. Simard, A. W. McConnachie, and J. T. Mendel. Galaxy pairs in the Sloan Digital Sky Survey - III. Evidence of induced star formation from optical colours. *MNRAS*, 412(1): 591–606, Mar. 2011. doi: 10.1111/j.1365-2966.2010.17932.x. 5
- Planck Collaboration, P. A. R. Ade, N. Aghanim, M. I. R. Alves, C. Armitage-Caplan, M. Arnaud, M. Ashdown, F. Atrio-Barandela, J. Aumont, H. Aussel, C. Baccigalupi, A. J. Banday, R. B. Barreiro, R. Barrena, M. Bartelmann, J. G. Bartlett, N. Bartolo, S. Basak, E. Battaner, R. Battye, K. Benabed, A. Benoît, A. Benoit-Lévy, J. P. Bernard, M. Bersanelli, B. Bertin-court, M. Bethermin, P. Bielewicz, I. Bikmaev, A. Blanchard, J. Bobin, J. J. Bock, H. Böhringer, A. Bonaldi, L. Bonavera, J. R. Bond, J. Borrill, F. R. Bouchet, F. Boulanger, H. Bourdin, J. W. Bowyer, M. Bridges, M. L. Brown, M. Bucher, R. Burenin, C. Burigana, R. C. Butler, E. Calabrese, B. Cappellini, J. F. Cardoso, R. Carr, P. Carvalho, M. Casale, G. Castex, A. Catalano, A. Challinor, A. Chamballu, R. R. Chary, X. Chen, H. C. Chiang, L. Y. Chiang, G. Chon, P. R. Christensen, E. Churazov, S. Church, M. Clemens, D. L. Clements, S. Colombi, L. P. L. Colombo, C. Combet, B. Comis, F. Couchot, A. Coulais, B. P. Crill, M. Cruz, A. Curto, F. Cuttaia, A. Da Silva, H. Dahle, L. Danese, R. D. Davies, R. J. Davis, P. de Bernardis, A. de Rosa, G. de Zotti, T. Déchelette, J. Delabrouille, J. M. Delouis, J. Démoclès, F. X. Désert, J. Dick, C. Dickinson, J. M. Diego, K. Dolag, H. Dole, S. Donzelli, O. Doré, M. Douspis, A. Ducout, J. Dunkley, X. Dupac, G. Efstathiou, F. Elsner, T. A. Enßlin, H. K. Eriksen, O. Fabre, E. Falgarone, M. C. Falvella, Y. Fantaye, J. Fergusson, C. Filliard, F. Finelli, I. Flores-Cacho, S. Foley, O. Forni, P. Fosalba, M. Frailis, A. A. Fraisse, E. Franceschi, M. Freschi, S. Fromenteau, M. Frommert, T. C. Gaier, S. Galeotta, J. Gallegos, S. Galli, B. Gandolfo, K. Ganga, C. Gauthier, R. T. Génova-Santos, T. Ghosh, M. Giard, G. Giardino, M. Gilfanov, D. Girard, Y. Giraud-Héraud, E. Gjerløw, J. González-Nuevo, K. M. Górski, S. Gratton, A. Gregorio, A. Gruppuso, J. E. Gudmundsson, J. Haissinski, J. Hamann, F. K. Hansen, M. Hansen, D. Hanson, D. L. Harrison, A. Heavens, G. Helou, A. Hempel, S. Henrot-Versillé, C. Hernández-Monteagudo, D. Herranz, S. R. Hildebrandt, E. Hivon, S. Ho, M. Hobson, W. A. Holmes, A. Hornstrup, Z. Hou, W. Hovest, G. Huey, K. M. Huffenberger, G. Hurier, S. Ilić, A. H. Jaffe, T. R. Jaffe, J. Jasche, J. Jewell, W. C. Jones, M. Juvela, P. Kalberla, P. Kangaslahti, E. Keihänen, J. Kerp, R. Kesitalo, I. Khamitov, K. Kiiveri, J. Kim, T. S. Kisner, R. Kneissl, J. Knoche, L. Knox, M. Kunz, H. Kurki-Suonio, F. Lacasa, G. Lagache, A. Lähtenmäki, J. M. Lamarre, M. Langer, A. Lasenby, M. Lattanzi, R. J. Laureijs, A. Lavabre, C. R. Lawrence, M. Le Jeune, S. Leach, and J. P. Leahy. Planck 2013 results. I. Overview of products and scientific results. *A&A*, 571:A1, Nov. 2014. doi: 10.1051/0004-6361/201321529. 3
- I. Ruffa, T. A. Davis, I. Prandoni, R. A. Laing, R. Paladino, P. Parma, H. de Ruiter, V. Casasola, M. Bureau, and J. Warren. The AGN fuelling/feedback cycle in nearby radio galaxies - II. Kinematics of the molecular gas. *MNRAS*, 489(3):3739–3757, Nov. 2019. doi: 10.1093/mnras/stz2368. 2
- V. M. Sampaio, A. Aragón-Salamanca, M. R. Merrifield, R. R. de Carvalho, S. Zhou, and I. Ferreras. The co-evolution of strong AGN and central galaxies in different environments. *MNRAS*, 524(4): 5327–5339, Oct. 2023. doi: 10.1093/mnras/stad2211. 2
- F. Santoro, C. Tadhunter, D. Baron, R. Morganti, and J. Holt. AGN-driven outflows and the AGN feedback efficiency in young radio galaxies. *A&A*, 644:A54, Dec. 2020. doi: 10.1051/0004-6361/202039077. 2

- S. Satyapal, S. L. Ellison, W. McAlpine, R. C. Hickox, D. R. Patton, and J. T. Mendel. Galaxy pairs in the Sloan Digital Sky Survey - IX. Merger-induced AGN activity as traced by the Wide-field Infrared Survey Explorer. *MNRAS*, 441(2):1297–1304, June 2014. doi: 10.1093/mnras/stu650. 2
- J. Schaye, R. A. Crain, R. G. Bower, M. Furlong, M. Schaller, T. Theuns, C. Dalla Vecchia, C. S. Frenk, I. G. McCarthy, J. C. Helly, A. Jenkins, Y. M. Rosas-Guevara, S. D. M. White, M. Baes, C. M. Booth, P. Camps, J. F. Navarro, Y. Qu, A. Rahmati, T. Sawala, P. A. Thomas, and J. Trayford. The EAGLE project: simulating the evolution and assembly of galaxies and their environments. *MNRAS*, 446(1): 521–554, Jan. 2015. doi: 10.1093/mnras/stu2058. 2, 3, 4, 13
- N. I. Shakura and R. A. Sunyaev. Black holes in binary systems. Observational appearance. *A&A*, 24: 337–355, Jan. 1973. 4
- J. Shangguan, L. C. Ho, F. E. Bauer, R. Wang, and E. Treister. AGN Feedback and Star Formation of Quasar Host Galaxies: Insights from the Molecular Gas. *ApJ*, 899(2):112, Aug. 2020. doi: 10.3847/1538-4357/aba8a1. 2
- A. Singh, C. Park, E. Choi, J. Kim, H. Jun, B. K. Gibson, Y. Kim, J. Lee, and O. Snaith. On the Effects of Local Environment on Active Galactic Nucleus (AGN) in the Horizon Run 5 Simulation. *ApJ*, 953 (1):64, Aug. 2023. doi: 10.3847/1538-4357/acdd6b. 2
- R. S. Somerville, P. F. Hopkins, T. J. Cox, B. E. Robertson, and L. Hernquist. A semi-analytic model for the co-evolution of galaxies, black holes and active galactic nuclei. *MNRAS*, 391(2):481–506, Dec. 2008. doi: 10.1111/j.1365-2966.2008.13805.x. 2
- V. Springel, T. Di Matteo, and L. Hernquist. Modelling feedback from stars and black holes in galaxy mergers. *MNRAS*, 361(3):776–794, Aug. 2005. doi: 10.1111/j.1365-2966.2005.09238.x. 2
- I. Strateva, Ž. Ivezić, G. R. Knapp, V. K. Narayanan, M. A. Strauss, J. E. Gunn, R. H. Lupton, D. Schlegel, N. A. Bahcall, J. Brinkmann, R. J. Brunner, T. Budavári, I. Csabai, F. J. Castander, M. Doi, M. Fukugita, Z. Györy, M. Hamabe, G. Hennessy, T. Ichikawa, P. Z. Kunszt, D. Q. Lamb, T. A. McKay, S. Okamura, J. Racusin, M. Sekiguchi, D. P. Schneider, K. Shimasaku, and D. York. Color Separation of Galaxy Types in the Sloan Digital Sky Survey Imaging Data. *AJ*, 122(4):1861–1874, Oct. 2001. doi: 10.1086/323301. 2
- J. W. Trayford, T. Theuns, R. G. Bower, J. Schaye, M. Furlong, M. Schaller, C. S. Frenk, R. A. Crain, C. Dalla Vecchia, and I. G. McCarthy. Colours and luminosities of $z = 0.1$ galaxies in the EAGLE simulation. *MNRAS*, 452(3):2879–2896, Sept. 2015. doi: 10.1093/mnras/stv1461. 3
- A. I. Visser-Zadvornyi, M. E. Carstairs, K. A. Oman, and M. A. W. Verheijen. Star formation and stellar & AGN feedback in the absence of accretion, not gas stripping, set the quenching time-scale in satellite galaxies. *MNRAS*, 540(2):1730–1744, June 2025. doi: 10.1093/mnras/staf802. 13
- A. Y. Wagner, M. Umemura, and G. V. Bicknell. Ultrafast Outflows: Galaxy-scale Active Galactic Nucleus Feedback. *ApJ Letters*, 763(1):L18, Jan. 2013. doi: 10.1088/2041-8205/763/1/L18. 2
- J.-H. Woo and C. M. Urry. Active Galactic Nucleus Black Hole Masses and Bolometric Luminosities. *ApJ*, 579(2):530–544, Nov. 2002. doi: 10.1086/342878. 2
- R. J. Wright, C. d. P. Lagos, L. J. M. Davies, C. Power, J. W. Trayford, and O. I. Wong. Quenching time-scales of galaxies in the EAGLE simulations. *MNRAS*, 487(3):3740–3758, Aug. 2019. doi: 10.1093/mnras/stz1410. 13

Z. Zhang, H. Wang, W. Luo, H. J. Mo, Z. Liang, R. Li, X. Yang, T. Wang, H. Zhang, H. Hong, X. Wang, E. Wang, P. Li, and J. Shi. Hosts and triggers of AGNs in the Local Universe. *A&A*, 650:A155, June 2021. doi: 10.1051/0004-6361/202040150. 2